Available online at www.sciencedirect.com
ScienceDirect
Nuclear Physics B Proceedings Supplement 00 (2014) 1–7
Nuclear Physics B Proceedings Supplement

Semileptonic B and B_s decays at Belle

Robin Glattauer[1]

Institute of High Energy Physics
Austrian Academy of Sciences
A-1050 Vienna, AUSTRIA

Abstract

Based on the large data sample accumulated by the Belle experiment at the KEKB asymmetric energy e^+e^- collider at KEK, Japan, we present new results on semileptonic $B_{(s)}$ meson decays.

The semileptonic decays $B \to X_c \ell \nu$ are the preferred modes for determining the Cabibbo-Kobayashi-Maskawa (CKM) matrix element $|V_{\rm cb}|$, a fundamental parameter of the Standard Model. The decay $B \to D\ell\bar{\nu}_\ell$ is measured for the first time with the full Belle data sample recorded at the $\Upsilon(4S)$ resonance. The preliminary result is $\eta_{\rm EW}\mathcal{G}(1)|V_{cb}| = (42.63 \pm 0.96_{\rm stat} \pm 1.39_{\rm syst}) \times 10^{-3}$ and $\rho^2 = 1.001 \pm 0.051_{\rm stat} \pm 0.018_{\rm syst}$ for the form factor parameter ρ^2.

Measurements of semileptonic B_s decays provide a test of QCD calculations entering the $|V_{\rm cb}|$ extraction. The heaviness of the s quark compared to the u and d quarks facilitates the theoretical description of B_s decays. We present preliminary results of branching fraction measurements of the semi-inclusive $B_s \to D_s^{(*)} X \ell \bar{\nu}_\ell$ decays: $\mathcal{B}(B_s \to D_s X \ell \nu) = (8.2 \pm 0.2_{\rm stat} \pm 0.8_{\rm syst} \pm 1.5_{N_{B_s}})\%$ and $\mathcal{B}(B_s \to D_s^* X \ell \nu) = (5.4 \pm 0.4_{\rm stat} \pm 0.5_{\rm syst} \pm 1.0_{N_{B_s}})\%$.

Keywords:
Belle, Vcb, semileptonic, hadronic tag, B, Bs

1. Introduction

There are two complementary approaches for measuring $|V_{\rm cb}|$ - inclusive and exclusive decays. In exclusive decays a specific charmed final state, e.g. D or D^*, is reconstructed. In inclusive decays all final states with a charm quark X_c are considered. Both the reconstruction and the theoretical descriptions differ, thus the systematic errors of the approaches can be seen as mostly independent.

Currently these two approaches yield different results for $|V_{\rm cb}|$, with the inclusive value being up to 3σ larger than the one from exclusive decays. See Table 1 for a comparison. This has lead to the question whether there are systematic errors in the experimental or theoretical procedure unaccounted for, or whether this is the result of physics beyond the standard model. This is especially interesting as in addition the sum of exclusive decays does not add up to the measured inclusive branching fraction - around 15% are missing.

Mode & model	$\lvert V_{\rm cb}\rvert$ $[10^{-3}]$
$B \to D^*\ell\bar{\nu}_\ell$, LQCD [1]	$39.54 \pm 0.50_{\rm exp} \pm 0.74_{\rm th}$
$B \to D^*\ell\bar{\nu}_\ell$, LQCD [2]	$39.04 \pm 0.49_{\rm exp} \pm 0.56_{\rm th}$
$B \to D^*\ell\bar{\nu}_\ell$, LCSR [3]	$41.47 \pm 0.52_{\rm exp} \pm 0.96_{\rm th}$
$B \to D\ell\bar{\nu}_\ell$, LQCD [4]	$39.44 \pm 1.42_{\rm exp} \pm 0.88_{\rm th}$
$B \to D\ell\bar{\nu}_\ell$, LCSR [5]	$40.73 \pm 1.46_{\rm exp} \pm 0.78_{\rm th}$
$B \to X_c\ell\bar{\nu}_\ell$[6]	42.42 ± 0.86

Table 1: $|V_{\rm cb}|$ results based on different measurements and theoretical models. The $B \to D^*\ell\bar{\nu}_\ell$ calculations use $\mathcal{F}(1)|V_{\rm cb}| = (35.90 \pm 0.11_{\rm stat} \pm 0.44_{\rm syst}) \times 10^{-3}$ and for $B \to D\ell\bar{\nu}_\ell$ a value of $\mathcal{G}(1)|V_{\rm cb}| = (42.64 \pm 0.72_{\rm stat} \pm 1.35_{\rm syst}) \times 10^{-3}$ was used. Both values are taken from the Heavy Flavor Averaging Group [7]. One can see that the exclusive values are systematically higher than the inclusive ones.

Email address: robin.glattauer@oeaw.ac.at (Robin Glattauer)

We present two measurements performed at the Belle experiment at the asymmetric electron positron collider KEKB [8]. First, we show the analysis of the decay $B \to D\ell\bar{\nu}_\ell$ which is used to measure $|V_{\rm cb}|$ and a form factor parameter ρ^2. Second, we determine the branching fractions of $B_s \to D_s^{(*)}X\ell\bar{\nu}_\ell$, which have never been measured directly before and offer both a verification of theoretical models and a preparation for future measurements of $B_s \to D_s^{(*)}\ell\bar{\nu}_\ell$.

2. Belle detector and data sets

The Belle detector is a large-solid-angle magnetic spectrometer that consists of a silicon vertex detector (SVD), a 50-layer central drift chamber (CDC), an array of aerogel threshold Cherenkov counters (ACC), a barrel-like arrangement of time-of-flight scintillation counters (TOF), and an electromagnetic calorimeter comprised of CsI(Tl) crystals (ECL) located inside a super-conducting solenoid coil that provides a 1.5 T magnetic field. An iron flux-return located outside of the coil is instrumented to detect K_L^0 mesons and to identify muons (KLM). The detector is described in detail elsewhere [9].

Over 1000 fb^{-1} data were recorded at Belle, of those are 703 fb^{-1} at the $\Upsilon(4S)$ resonance which decays dominantly into a $B\bar{B}$ pair and 121 fb^{-1} at the $\Upsilon(5S)$ resonance which can also decay into a $B_s\bar{B}_s$ pair.

3. $B \to D\ell\bar{\nu}_\ell$

There are two exclusive decays with a branching fraction high enough to determine $|V_{\rm cb}|$: $B \to D^*\ell\bar{\nu}_\ell$ and $B \to D\ell\bar{\nu}_\ell$. While the former is preferred because of low backgrounds and high yields which results in a good precision, $B \to D\ell\bar{\nu}_\ell$ allows independent verification and by using hadronic tagging can come close to the precision of $B \to D^*\ell\bar{\nu}_\ell$.

We present the preliminary measurement of $B \to D\ell\bar{\nu}_\ell$ with the full Belle data sample of 703 fb^{-1} at the $\Upsilon(4S)$ resonance. This is the first time $B \to D\ell\bar{\nu}_\ell$ is measured at Belle using hadronic tagging. This method has been used before at the BaBar experiment [10].

3.1. Theory

The determination of the CKM matrix element $|V_{\rm cb}|$ is based on semileptonic B decays [11]. The theoretical description of semileptonic decays takes advantage of the large mass of the W-boson relative to the energies relevant in $B \to X_c\ell\bar{\nu}_\ell$ ($m_W \gg m_b$) and allows to integrate over the dynamic degrees of freedom of the W boson at tree-level, leading to a Fermi-like Hamiltonian:

$$\mathcal{H} = \frac{G_F}{\sqrt{2}} V_{cb}\,(\bar{c}\gamma_\mu(1-\gamma_5)b)(\ell\gamma^\mu(1-\gamma_5)\nu_\ell)\,, \quad (1)$$

Residual electroweak interactions between the hadronic and leptonic current are usually taken into account by introducing an electroweak correction factor $\eta_{\rm EW}$ (e.g. $\eta_{\rm EW} = 1.0066$ from [12]).

The leptonic current can be calculated perturbatively with QED while the main theoretical challenge is the description of the hadronic current, which can be treated e.g. in the frameworks of Lattice QCD (LQCD) or Light Cone Sum Rules (LCSR).

Parameterizing the hadronic current of the Hamiltonian with a form factor $\mathcal{G}(w)$ [13], one obtains the differential decay width of $B \to D\ell\bar{\nu}_\ell$:

$$\frac{d\Gamma}{dw} = \frac{G_F^2 m_D^3}{48\pi^3}(m_B + m_D)^2(w^2-1)^{3/2} \\ |\eta_{\rm EW}|^2|V_{\rm cb}|^2|\mathcal{G}(w)|^2\,, \quad (2)$$

where w is the product of the 4-velocities of the B and D meson:

$$w = v_B \cdot v_D = \frac{M_B^2 + M_D^2 - q^2}{2M_BM_D}\,. \quad (3)$$

and ranges from 1.0 to ~ 1.6.

Using the parameterization by Caprini *et al.* [14], the form factor can be approximated as

$$\mathcal{G}(w) = \mathcal{G}(1)(1 - 8\rho^2 z + (51\rho^2 - 10)z^2 - (252\rho^2 - 84)z^3)\,, \quad (4)$$

with

$$z = \frac{\sqrt{w+1} - \sqrt{2}}{\sqrt{w+1} + \sqrt{2}}\,. \quad (5)$$

The decay width is expressed in terms of two parameters, $\eta_{\rm EW}\mathcal{G}(1)|V_{cb}|$ and ρ^2. $\mathcal{G}(1)$ is the form factor at zero recoil and $\eta_{\rm EW}$ is the aforementioned electroweak correction factor. The current status of the art is to measure $\eta_{\rm EW}\mathcal{G}(1)|V_{cb}|$ and to calculate $\eta_{\rm EW}$ and $\mathcal{G}(1)$ in the theoretical frameworks in order to extract $|V_{\rm cb}|$.

3.2. Hadronic tagging

Hadronic tagging at the $\Upsilon(4S)$ resonance aims at the full reconstruction of one B meson ($B_{\rm tag}$) in a hadronic mode. This reduces combinatorial background when reconstructing the second B meson and constrains its kinematics.

The newest version of hadronic tagging at Belle applies a neural network based algorithm [15]. Compared to previous cut based approaches this results in twice the efficiencies - 0.28 % for $B^{\pm}$ and 0.18 % for B^0, with over 1000 different exclusive hadronic decay channels being reconstructed.

These channels include B mesons decaying to $D^{(*)}_{(s)}$ or J/ψ, either as pairs (e.g. $B^- \to D^0 D_s^-$) or in combination with kaons and pions (e.g. $J/\psi \to J/\psi K^- \pi^+ \pi^-$).

3.3. Reconstruction and extraction of $|V_{\rm cb}|$

The CKM matrix element $|V_{\rm cb}|$ is determined independently in 4 disjunct samples, separating electrons and muons, as well as charged and neutral B mesons. The results of the 4 samples are then averaged for a final result taking into account correlations between the samples.

$B \to D\ell\bar{\nu}_\ell$ is reconstructed in events with a hadronic tag from the charged tracks and neutral energy measurements not already assigned to $B_{\rm tag}$. This reduces the combinatorial background to a very high degree. Lepton candidates are charged tracks with a sufficiently high likelihood of being an electron or muon based on the particle identification possibilities of the Belle detector.

The D meson is reconstructed in one of 15 hadronic decay channels, for D^+: $K^-\pi^+\pi^+$, $K^-\pi^+\pi^+\pi^0$, $K^0_s\pi^+$, $K^0_s\pi^+\pi^0$, $K^+K^-\pi^+$, $K^0_sK^+$, $K^0_s\pi^+\pi^+\pi^-$, and for D^0: $K^-\pi^+$, $K^-\pi^+\pi^0$, $K^-\pi^+\pi^+\pi^-$, $K^0_s\pi^+\pi^-$, $K^0_s\pi^+\pi^-\pi^0$, $K^0_s\pi^0$, K^+K^-, $\pi^+\pi^-$.

One then compares the 4-momenta of the reconstructed particles to the known 4-momentum of the electron-positron beam and calculates the square of the invariant missing mass:

$$M^2_{\rm miss} = (p_{\rm beam} - p_{B_{\rm tag}} - p_D - p_\ell)^2 \,, \qquad (6)$$

For a genuinely reconstructed decay the only missing momentum belongs to the undetectable neutrino and one expects $M^2_{\rm miss}$ to be equal to the neutrino mass of approximately 0, see for example Fig. 1.

We use this distinct shape to separate signal from background. The main background sources are $B \to D^*\ell\bar{\nu}_\ell$ decays and erroneous tag side reconstructions. A binned extended maximum likelihood fit [16] is used to extract the number of signal events. We model the different components with Monte Carlo templates and leave signal, background from $B \to D^*\ell\bar{\nu}_\ell$ and wrong tags floating while other smaller backgrounds (e.g. fake or non-prompt leptons) are fixed to their Monte Carlo expectations. All in all we reconstruct 14057 signal events. A fit in a subrange of w in the sample $\bar{B}^0 \to D^+e^-\bar{\nu}_\ell$ can be seen in Fig. 2.

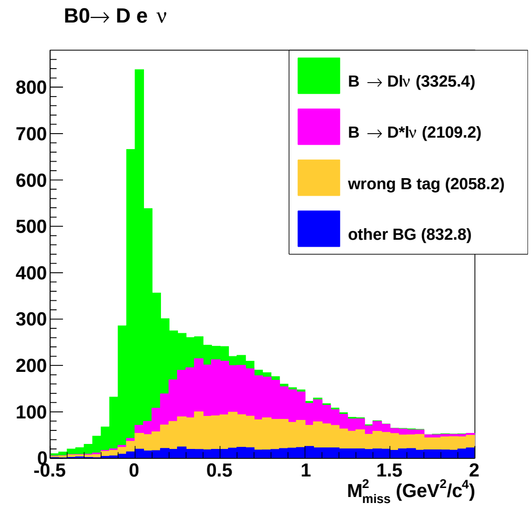

Figure 1: The $M^2_{\rm miss}$distribution of the sample $\bar{B}^0 \to D^+e^-\bar{\nu}_\ell$ for Monte Carlo simulated events.

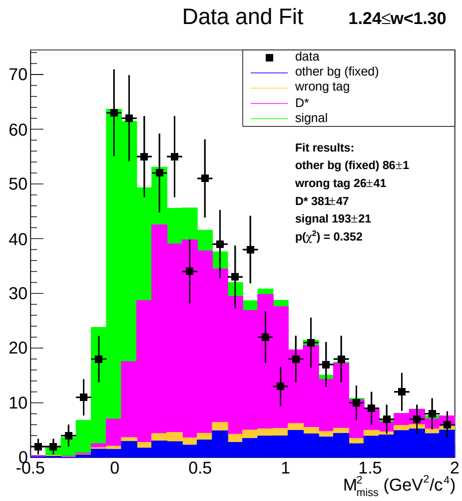

Figure 2: The yield fit for the range $1.24 \leq w < 1.30$ in the sample $\bar{B}^0 \to D^+e^-\bar{\nu}_\ell$.

Given equations 2-5 one can predict the signal yields for a given value of $\eta_{\rm EW}\mathcal{G}(1)|V_{cb}|$, ρ^2 and w. We perform signal yield measurements in 10 bins of w and extract $\eta_{\rm EW}\mathcal{G}(1)|V_{cb}|$ and ρ^2 via a χ^2 fit to the resulting distribution. This is shown in Fig. 3 for the sample $\bar{B}^0 \to D^+e^-\bar{\nu}_\ell$.

3.4. Results

Table 2 and Fig. 4 show the results of the fits for the 4 subsamples and their average. Comparing the results to those of the $B \to D\ell\bar{\nu}_\ell$ measurement with hadronic tagging at BaBar [10] we see a perfect agreement of $|V_{\rm cb}|$,

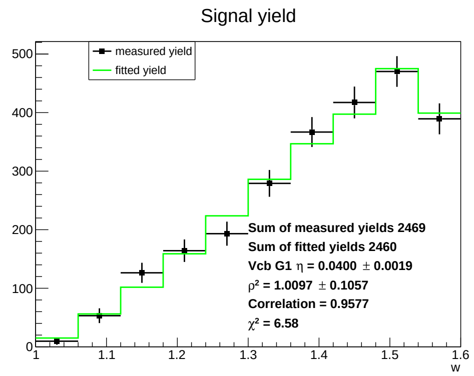

Figure 3: The χ^2 fit of $\eta_{\rm EW}\mathcal{G}(1)|V_{cb}|$ and ρ^2 in the sample $\bar{B}^0 \to D^+e^-\bar{\nu}_\ell$.

but the ρ^2 measured by Belle is about 2σ smaller than that of BaBar. The reduced ρ^2 leads to higher branching fractions of $\mathcal{B}(\bar{B}^0 \to D^+\ell^-\bar{\nu}_\ell) = (2.49 \pm 0.17)\%$ and $\mathcal{B}(B^- \to \bar{D}^0\ell^-\bar{\nu}_\ell) = (2.70 \pm 0.19)\%$ which would close $\sim 20\%$ of the gap between inclusive and exclusive branching fractions.

The main sources of systematic errors for $\eta_{\rm EW}\mathcal{G}(1)|V_{cb}|$ are the calibration of the hadronic tagging with a relative error of 2.9 %, the efficiencies of charged track reconstruction (1.75 %) and the branching fractions of background events (1.51 %).

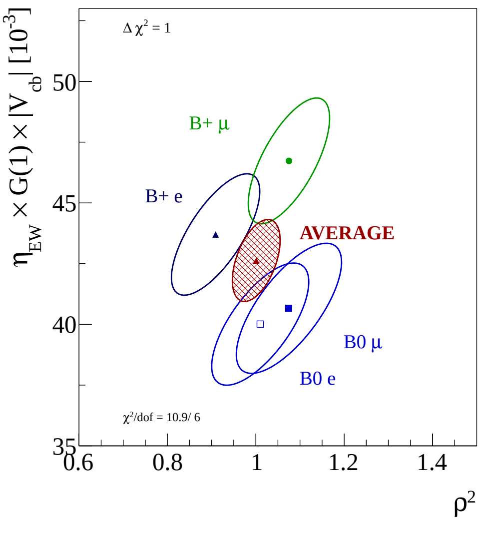

Figure 4: Results of $\eta_{\rm EW}\mathcal{G}(1)|V_{cb}|$ and ρ^2 extraction with $B \to D\ell\bar{\nu}_\ell$. The ellipses show the two dimensional $1\,\sigma$ contour.

4. $B_s \to D_s^{(*)}X\ell\bar{\nu}_\ell$

Besides the 703 fb^{-1} of data taken at the $\Upsilon(4S)$ resonance, Belle also gathered 121 fb^{-1} at the $\Upsilon(5S)$ resonance which by its higher energy allows production of $B_s\bar{B}_s$ pairs. This $\Upsilon(5S)$ sample allows detailed studies of B_s meson decays.

B_s mesons offer different advantages compared to B mesons, such as easier theoretical description due to the higher mass of the spectator quark. B_s measurements are very useful to verify the results from B measurements and to test the predictions of QCD calculations. On the other hand, in contrast to $\Upsilon(4S)$ only $(17.2 \pm 3.0)\%$ [17] of the $\Upsilon(5S)$ resonances decay into $B_s\bar{B}_s$ pairs, the rest into $B\bar{B}$ pairs.

Different semileptonic decays of the B_s have been studied, e.g. $B_s \to X\ell\nu$ at Babar [18] and Belle [19], $\mathcal{B}(\bar{b} \to B_s)\cdot\mathcal{B}(B_s \to D_s^{(*)}X\ell\bar{\nu}_\ell)$ at LEP [20, 21, 22] or $\bar{B}_s^0 \to D_{s2}^{*+}X\mu^-\bar{\nu}$ at LHCb [23].

The modes $B_s \to D_s^{(*)}\ell\bar{\nu}_\ell$ have not been measured so far. We present the first measurement of the semi-inclusive decays $B_s \to D_s^{(*)}X\ell\bar{\nu}_\ell$, where X stands for zero or more additional particles.

Assuming little down-feed from higher excited states D_s^{**} to D_s^*, the $B_s \to D_s^*X\ell\bar{\nu}_\ell$ branching fraction can be interpreted as $B_s \to D_s^*\ell\bar{\nu}_\ell$ branching fraction. The $B_s \to D_sX\ell\bar{\nu}$ measurement on the other hand allows in particular to draw conclusions about the $B_s \to D_s^{**}(D^{(*)}K)\ell\bar{\nu}$ branching fractions without explicitly reconstructing the D_s^{**} states. Assuming that these are the dominant sources of $D^{(*)}$ mesons from semileptonic B_s decays their size can be estimated by calculating $\mathcal{B}(B_s \to X\ell\bar{\nu}) - \mathcal{B}(B_s \to D_sX\ell\bar{\nu})$.

4.1. Reconstruction

The analysis is based on reconstructed $D_s^-\ell^+$ and $D_s^{*-}\ell^+$ pairs. D_s mesons are reconstructed in the clean decay mode to $\phi(K^+K^-)\pi^-$ and D_s^* mesons are reconstructed in their dominant mode $D_s^* \to D_s\gamma$ by adding a reconstructed photon to a D_s. Combinatorial background is reduced by applying a mass range for the ϕ meson: $1004\,\text{MeV}/c^2 \leq m_\phi \leq 1034\,\text{MeV}/c^2$. For the D_s meson a wide range of $1903.5\,\text{MeV}/c^2 \leq m_{D_s} \leq 2033.5\,\text{MeV}/c^2$ is applied containing enough side bands to allow fitting. The $D_s^{(*)}$ mesons are then combined with a lepton of opposite charge.

The number of genuinely reconstructed D_s and D_s^* mesons can be measured by fits to the distribution of the reconstructed D_s mass; or for the D_s^* by fitting $\Delta m = m_{D_s^*} - m_{D_s}$, see Fig. 6 and 7. The shape of genuine D_s is modeled with a sum of two Gaussian functions with a common mean and the background is modeled

Sample	$\eta_{\rm EW}\mathcal{G}(1)\lvert V_{cb}\rvert[10^{-3}]$	ρ^2	correlation
$\bar{B}^0 \to D^+e^-\bar{\nu}_\ell$	$40.01 \pm 1.89_{\rm stat} \pm 1.66_{\rm syst}$	$1.010 \pm 0.106_{\rm stat} \pm 0.029_{\rm syst}$	0.692
$\bar{B}^0 \to D^+\mu^-\bar{\nu}_\ell$	$40.66 \pm 2.07_{\rm stat} \pm 1.70_{\rm syst}$	$1.075 \pm 0.115_{\rm stat} \pm 0.031_{\rm syst}$	0.713
$B^- \to \bar{D}^0e^-\bar{\nu}_\ell$	$43.70 \pm 1.86_{\rm stat} \pm 1.67_{\rm syst}$	$0.909 \pm 0.099_{\rm stat} \pm 0.014_{\rm syst}$	0.711
$B^- \to \bar{D}^0\mu^-\bar{\nu}_\ell$	$46.73 \pm 1.87_{\rm stat} \pm 1.79_{\rm syst}$	$1.075 \pm 0.091_{\rm stat} \pm 0.014_{\rm syst}$	0.680
Average	$42.63 \pm 0.96_{\rm stat} \pm 1.39_{\rm syst}$	$1.001 \pm 0.051_{\rm stat} \pm 0.018_{\rm syst}$	0.494

Table 2: Results of $\eta_{\rm EW}\mathcal{G}(1)\lvert V_{cb}\rvert$ and ρ^2 extraction with $B \to D\ell\bar{\nu}_\ell$.

with a first order Chebychev polynomial. The PDF of D_s^* is modeled with a sum of a Gaussian function and a Crystal Ball function with a common mean and for misreconstructed D_s^* a third order Chebychev polynomial is used.

4.2. Branching fraction extraction

Events containing a true $D_s^{(*)}$ meson can be organized in five categories: 1. background from $c\bar{c}$ continuum events, 2. $B_s \to D_s^{(*)}K\ell\nu$ events, 3. wrong-side combinations where the $D_s^{(*)}$ meson and the lepton candidate stem from different B_s decays, 4. other background where the lepton candidate stems either from a secondary decay or is a misreconstructed hadron, 5. signal decays comprising $D_s\ell\bar{\nu}$, $D_s^*\ell\bar{\nu}$ and $D_s^{**}\ell\bar{\nu}$.

Background (1) is determined from an off-resonance data sample and background (2) is estimated from MC simulation. The normalization of the remaining backgrounds and the signal component is determined by dividing the data sample in three regions according to the decay kinematics and comparing the MC expectations to the data event yields in each region. The regions are defined using the lepton momentum p_ℓ^* and the variable

$$X_{\rm mis} = \frac{(E_B^* - E_{\rm vis}^*) - p_{\rm vis}^*}{p_B^*}, \quad (7)$$

with

$$p_{\rm vis}^* = |\vec{p}_\ell^{\,*} + \vec{p}_D^{\,*}|, \quad (8)$$

$$E_{\rm vis}^* = E_\ell^* + E_D^* \quad (9)$$

Fig. 5 shows the $X_{\rm mis}$ distribution of correctly reconstructed D_s mesons in the $B_s \to D_sXe\nu$ sample. Signal events peak in the region $X_{\rm mis} > -1$.

The reconstructed events are separated into 3 distinct regions, each of which enhances a certain component:

A $X_{\rm mis} < -1$ enhances wrong side background

B $X_{\rm mis} > -1$, $p^* < 1.4\,{\rm GeV}/c$ enhances other background

C $X_{\rm mis} > -1$, $p^* > 1.4\,{\rm GeV}/c$ enhances signal

The separation can be seen in Fig. 5. The signal and the two remaining background components (3 and 4) form 3 degrees of freedom. Counting the events in each region constitutes 3 equations, which can be solved in order to determine the signal yields.

If we assume that the 3 components have the same distribution as in the Monte Carlo, but a different overall scale factor, the number of events in each region can be calculated to be:

$$N_i^{\rm Data} = \sum_j a_j N_{i,j}^{\rm MC}, \quad (10)$$

where i denotes the region and j the component. a_j are the scale factors for each component. These scale factors can be calculated using a χ^2 fit with:

$$\chi^2 = \sum_i \frac{(N_i^{\rm Data} - \sum_j a_j N_{i,j}^{\rm MC})^2}{(\Delta N_i^{\rm Data})^2 + (\sum_j a_j \Delta N_{i,j}^{\rm MC})^2} \quad (11)$$

The resulting signal yields are then:

$$N_{\rm signal} = \sum_i a_{\rm signal} N_{i,\rm signal}^{\rm MC} \quad (12)$$

From the number of signal events the branching fraction can be calculated by:

$$\mathcal{B} = \frac{N_{\rm signal}}{\epsilon \cdot \mathcal{B}(D_s^- \to \phi(K^+K^-)\pi^-) \cdot N_{B_s}}, \quad (13)$$

where ϵ is the efficiency of the reconstruction and N_{B_s} is the number of B_s mesons.

4.3. Results

The preliminary results of the branching fractions obtained can be seen in Table 3. The dominant source of systematic error is the number of B_s mesons produced at the $\Upsilon(5S)$ resonance at Belle and is thus listed separately. Other sources include $\mathcal{B}(D_s \to \phi\pi; \phi \to K^+K^-)$ with a relative error of 5.3 %, the impact of signal and background modeling on the yield measurements (3-5 %) and detection efficiencies and fake rates (2.5-3.4 %).

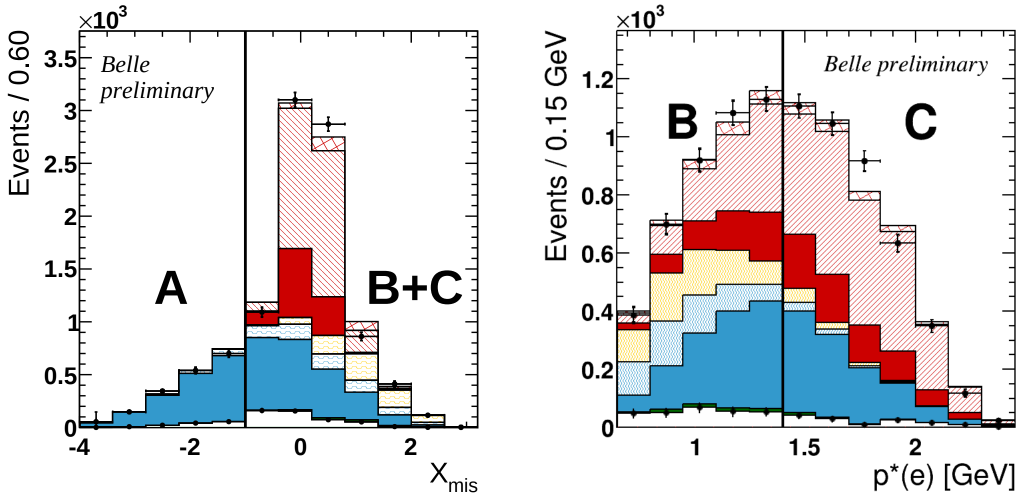

Figure 5: X_{mis} and lepton momentum in the center of mass frame for the sample $B_s \to D_s X e\nu$. White is continuum background, green $B_s \to D_s^{(*)} K \ell \nu$ decays, blue describes different kinds of wrong side background while yellow contains "other background" and red denotes the various signal components: solid red is $B_s \to D_s \ell \bar{\nu}$, hatched red is $B_s \to D_s^{*} \ell \bar{\nu}$ and crosshatched red is $B_s \to D_s^{**} \ell \bar{\nu}$. The letters "A","B" and "C" denote the 3 signal regions used in the counting experiment.

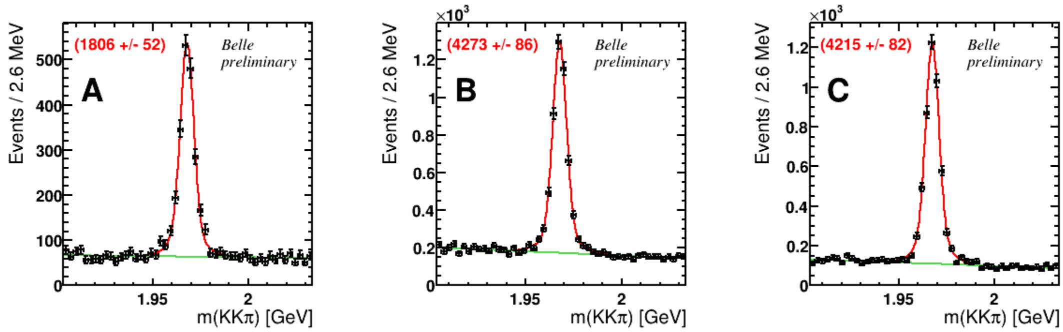

Figure 6: Fit to the D_s mass in the three different regions of the sample $B_s \to D_s X e\nu$

Comparing these results to recent theoretical estimations of $B_s \to D_s^{(*)} \ell \bar{\nu}_\ell$ from [24] with $\mathcal{B}(B_s \to D_s X \ell \nu) = 2.1 \pm 0.2$ and $\mathcal{B}(B_s \to D_s^* X \ell \nu) = 5.3 \pm 0.5$, or from [25] with $\mathcal{B}(B_s \to D_s X \ell \nu) = 1.55 \pm 0.15$ and $\mathcal{B}(B_s \to D_s^* X \ell \nu) = 5.45 \pm 0.35$ we see that the results are compatible with theory predictions within the experimental uncertainty and hint at a small branching fraction of $B_s \to D_s^{**} \ell \nu_\ell$.

The result on $B_s \to D_s X \ell \nu$ also agrees with the small $B_s \to D_s^{**}(D^{(*)}K) \ell \bar{\nu}$ branching fractions as measured by D0 [26] and LHCb [23].

5. Conclusion

We presented two new preliminary measurements at the Belle experiment which explore the semileptonic decays of $B_{(s)}$ mesons.

$B \to D \ell \bar{\nu}_\ell$ was used to determine $\eta_{\text{EW}} \mathcal{G}(1)|V_{cb}|$ and the form factor parameter ρ^2. The result for $\eta_{\text{EW}} \mathcal{G}(1)|V_{cb}| = (42.63 \pm 0.96_{\text{stat}} \pm 1.39_{\text{syst}}) \times 10^{-3}$ is perfectly compatible with previous measurements by BaBar, while the result for $\rho^2 = 1.001 \pm 0.051_{\text{stat}} \pm 0.018_{\text{syst}}$ differs at a level of 2σ, which raises $\mathcal{B}(B \to D \ell \bar{\nu}_\ell)$ and reduces the branching fraction gap of inclusive and exclusive measurements.

The branching fractions of the semi-inclusive decays $B_s \to D_s^{(*)} X \ell \bar{\nu}_\ell$ were measured to be $\mathcal{B}(B_s \to D_s X \ell \nu) = (8.2 \pm 0.2_{\text{stat}} \pm 0.8_{\text{syst}} \pm 1.5_{N_{B_s}})\%$ and $\mathcal{B}(B_s \to D_s^* X \ell \nu) = (5.4 \pm 0.4_{\text{stat}} \pm 0.5_{\text{syst}} \pm 1.0_{N_{B_s}})\%$. These results were directly measured for the first time and are in good agreement with theoretical predictions and measurements of other semileptonic B_s decays.

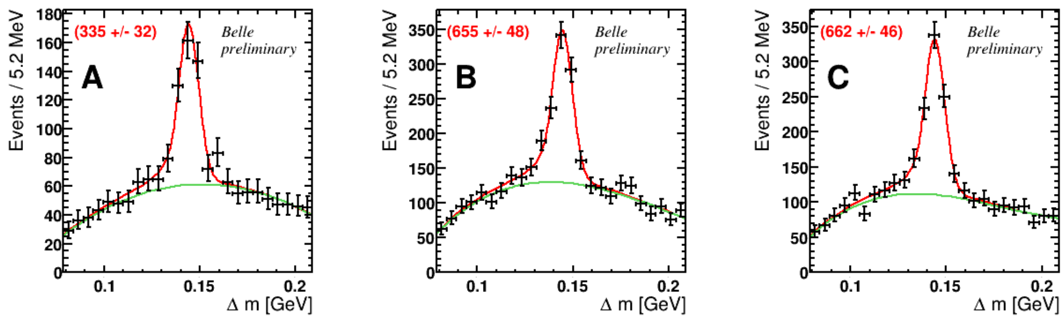

Figure 7: Fit to Δm in the three different regions of the sample $B_s \to D_s^* X e\nu$

sample	$\mathcal{B}$ [%]
$B_s \to D_s X e\nu$	$8.2 \pm 0.3_{\mathrm{stat}} \pm 0.7_{\mathrm{syst}} \pm 1.5_{N_{B_s}}$
$B_s \to D_s X \mu\nu$	$8.3 \pm 0.3_{\mathrm{stat}} \pm 0.8_{\mathrm{syst}} \pm 1.5_{N_{B_s}}$
$B_s \to D_s^* X e\nu$	$5.2 \pm 0.6_{\mathrm{stat}} \pm 0.5_{\mathrm{syst}} \pm 0.9_{N_{B_s}}$
$B_s \to D_s^* X \mu\nu$	$5.8 \pm 0.6_{\mathrm{stat}} \pm 0.6_{\mathrm{syst}} \pm 1.0_{N_{B_s}}$
$B_s \to D_s X \ell\nu$	$8.2 \pm 0.2_{\mathrm{stat}} \pm 0.8_{\mathrm{syst}} \pm 1.5_{N_{B_s}}$
$B_s \to D_s^* X \ell\nu$	$5.4 \pm 0.4_{\mathrm{stat}} \pm 0.5_{\mathrm{syst}} \pm 1.0_{N_{B_s}}$

Table 3: Preliminary branching fractions of $B_s \to D_s^{(*)} X \ell \bar{\nu}_\ell$ decays measured separately for electrons and muons. The combinations of the measurements take into account the correlations between the two modes.

References

[1] J. A. Bailey, et al., $B \to D^* \ell \nu$ at zero recoil: an update, PoS LATTICE2010 (2010) 311. arXiv:1011.2166.

[2] J. A. Bailey, et al., Update of $|V_{cb}|$ from the $\bar{B} \to D^* \ell \bar{\nu}$ form factor at zero recoil with three-flavor lattice QCD, Phys.Rev. D89 (2014) 114504. arXiv:1403.0635.

[3] P. Gambino, et al., $B \to D^*$ at zero recoil revisited, Phys.Rev. D81 (2010) 113002. arXiv:1004.2859.

[4] M. Okamoto, et al., Semileptonic $D \to \pi/K$ and $B \to \pi/D$ decays in 2+1 flavor lattice QCD, Nucl.Phys.Proc.Suppl. 140 (2005) 461–463. arXiv:hep-lat/0409116.

[5] N. Uraltsev, A 'BPS' expansion for B and D mesons, Phys.Lett. B585 (2004) 253–262. arXiv:hep-ph/0312001.

[6] P. Gambino, C. Schwanda, Inclusive semileptonic fits, heavy quark masses, and V_{cb}, Phys.Rev. D89 (2014) 014022. arXiv:1307.4551.

[7] Y. Amhis, et al., Averages of B-Hadron, C-Hadron, and tau-lepton properties as of early 2012. arXiv:1207.1158.

[8] S. Kurokawa, Overview of the KEKB accelerators, Nucl.Instrum.Meth. A499 (2003) 1–7.

[9] A. Abashian, K. Gotow, N. Morgan, L. Piilonen, S. Schrenk, et al., The Belle Detector, Nucl.Instrum.Meth. A479 (2002) 117–232.

[10] B. Aubert, et al., Measurement of $|V_{cb}|$ and the Form-Factor Slope in $\bar{B} \to D\ell\bar{\nu}$ Decays in Events Tagged by a Fully Reconstructed B Meson, Phys.Rev.Lett. 104 (2010) 011802. arXiv:0904.4063.

[11] K. Olive, et al., Review of Particle Physics, Chin.Phys. C38 (2014) 090001.

[12] A. Sirlin, Large m_W, m_Z behaviour of the $O(\alpha)$ corrections to semileptonic processes mediated by W, Nuclear Physics B 196 (1) (1982) 83–92.

[13] M. Neubert, Model-independent extraction of V_{cb} from semi-leptonic decays, Physics Letters B 264 (3) (1991) 455–461.

[14] I. Caprini, L. Lellouch, M. Neubert, Dispersive bounds on the shape of $B \to D^{(*)} \ell \nu$ form factors, Nuclear Physics B 530 (1) (1998) 153–181.

[15] M. Feindt, et al., A Hierarchical NeuroBayes-based Algorithm for Full Reconstruction of B Mesons at B Factories, Nucl.Instrum.Meth. A654 (2011) 432–440. arXiv:1102.3876.

[16] R. Barlow, C. Beeston, Fitting using finite monte carlo samples, Computer Physics Communications 77 (2) (1993) 219–228.

[17] This number was obtained by the Belle Collaboration with the method described in:
A. Drutskoy, et al., Measurement of inclusive $D_{(s)}$, D^0 and J/ψ rates and determination of the $B^*_{(s)}$ anti-$B^*_{(s)}$ production fraction in b anti-b events at the $\Upsilon(5S)$ resonance, Phys.Rev.Lett. 98 (2007) 052001. arXiv:hep-ex/0608015.

[18] J. Lees, et al., A Measurement of the Semileptonic Branching Fraction of the B_s Meson, Phys.Rev. D85 (2012) 011101. arXiv:1110.5600.

[19] C. Oswald, et al., Measurement of the inclusive semileptonic branching fraction $\mathcal{B}(B_s^0 \to X^- \ell^+ \nu_\ell)$ at Belle, Phys.Rev. D87 (7) (2013) 072008. arXiv:1212.6400.

[20] D. Buskulic, et al., Measurement of $D^+_{(s)}$ meson production in Z decays and of the anti-$B^0_{(s)}$ lifetime, Z.Phys. C69 (1996) 585–596.

[21] P. Acton, et al., Evidence for the existence of the strange b flavored meson B_s^0 in Z^0 decays, Phys.Lett. B295 (1992) 357–370.

[22] P. Abreu, et al., Evidence for B_s^0 meson production in Z^0 decays, Phys.Lett. B289 (1992) 199–210.

[23] R. Aaij, et al., First observation of $\bar{B}_s^0 \to D_{s2}^{*+} X \mu^- \bar{\nu}$ decays, Phys.Lett. B698 (2011) 14–20. arXiv:1102.0348.

[24] R. Faustov, V. Galkin, Weak decays of B_s mesons to D_s mesons in the relativistic quark model, Phys.Rev. D87 (2013) 034033. arXiv:1212.3167.

[25] X. Chen, et al., Estimating Form Factors of $B_s \to D_s^{(*)}$ and their Applications to Semi-leptonic and Non-leptonic Decays, J.Phys. G39 (2012) 045002. arXiv:1106.3003.

[26] V. Abazov, et al., Measurement of the B_s^0 semileptonic branching ratio to an orbitally excited D_s state, Br($B_s^0 \to D_{s1}^-(2536) \mu^+ \nu X$), Phys.Rev.Lett. 102 (2009) 051801. arXiv:0712.3789.